

Multi-photon scattering tomography with coherent states

Tomás Ramos and Juan José García-Ripoll

Instituto de Física Fundamental IFF-CSIC, Calle Serrano 113b, Madrid 28006, Spain

(Dated: September 27, 2022)

In this work we develop an experimental procedure to interrogate the single- and multi-photon scattering matrices of an unknown quantum object interacting with propagating photons. Our proposal requires coherent state laser or microwave inputs and homodyne detection at the scatterer's output, and provides simultaneous information about multiple —elastic and inelastic— segments of the scattering matrix. The method is resilient to detector noise and its errors can be made arbitrarily small by combining experiments at various laser powers. Finally, we show that the tomography of scattering has to be performed using pulsed lasers to optimally gather information about the nonlinear processes in the scatterer.

PACS numbers: 03.65.Nk, 42.50.-p, 72.10.F1

It is now possible to achieve strong and ultrastrong coupling between quantum emitters and propagating photons using superconducting qubits [1–4], atoms [5, 6] or quantum dots [7] in photonic circuits, or even molecules in free space [8]. This has motivated a stunning progress in the theory of single- and multi-photon scattering using wavefunctions [9] and Bethe ansatz [10], as well as input-output theory [11, 12], diagrammatic calculations [13–15], and path integral formalism [16, 17]. Very recently, the theory has even covered the ultrastrong coupling regime [18]. Experiments, however, cannot yet recover all the scattering information predicted by those studies, and are limited to comparing low-power coherent state transmission coefficients [1, 4, 19], cross-Kerr phases [3], and antibunching [2]. We therefore need an ambitious framework for reconstructing the complete one-, two-, or ideally any multi-photon scattering matrix. Such framework would allow studying the elastic [20], and inelastic [21] properties of quantum impurities in waveguides, quasi-particle spectroscopy [22], interactions [23] in quantum simulators, and even characterizing all-optical quantum processors.

In this Letter we present a theoretical and experimental framework for estimating the scattering matrix that describes the transition amplitude from an input state of m photons with momenta k_1, \dots, k_m , to an asymptotic output state of n photons with momenta p_1, \dots, p_n [cf. Fig. 1a], as

$$S_{p_1 \dots p_n k_1 \dots k_m} = \langle 0 | A_{p_1} \dots A_{p_n} U A_{k_1}^\dagger \dots A_{k_m}^\dagger | 0 \rangle. \quad (1)$$

Operator U represents the evolution in the limit of infinitely long time, and A_k^\dagger are generic input and output bosonic operators that create a photon on top of the vacuum state $|0\rangle$. Our proposal assumes an experimental setup where we can inject coherent states and perform homodyne detection at the output of a generalized multi-port beam-splitter [cf. Fig. 1b]. Through a clever combination of measurements with different input phases and amplitudes, we can approximate (1) with arbitrarily small error. In addition, our scheme is ide-

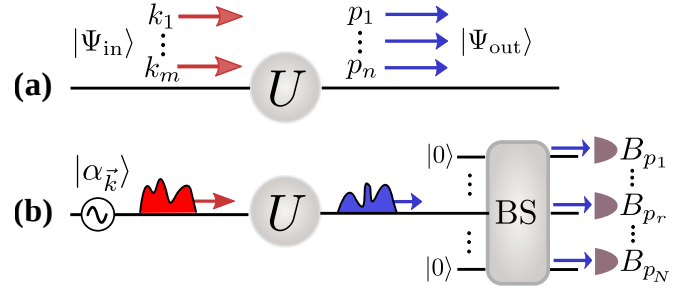


FIG. 1. (a) A quantum scatterer with scattering matrix U transforms an input state $|\Psi_{\text{in}}\rangle$ of m photons with momenta k_1, \dots, k_m into an outgoing state $|\Psi_{\text{out}}\rangle = U|\Psi_{\text{in}}\rangle$ of n photons with momenta, p_1, \dots, p_n . (b) Our experimental protocol for determining U requires coherent state wavepackets inputs $|\alpha_{\vec{k}}\rangle$, prepared with a signal generator (\sim), and homodyne measurements at the output. Prior to measurement, the output signal is split evenly by an N -port beam-splitter (BS), so as to filter the momenta in the correlations $\langle B_{p_1} \dots B_{p_n} \rangle$.

ally suited for superconducting circuits and nanophotonics experiments, because all noise from amplifiers or detectors is canceled without previous calibration, similar to the dual-path method [24–26]. In this Letter we also prove that an accurate reconstruction of the scattering matrix demands the use of finite length input wavepackets A_k^\dagger , engineered to optimally probe the nonlinear contributions to the photon dynamics. However, standard deconvolution techniques allow us to also infer the scattering matrix elements in the monochromatic limit of Eq. (1). We exemplify this idea using a two-level scatterer, for which we have accurate analytical results [11], and experiments have already been performed at the single-photon level [1, 2]. This work is closed with a discussion on the generality of the protocol, and possible implementations in state-of-the-art setups.

Scattering tomography ingredients: We present our scheme beginning with (i) the tomography architecture, (ii) a discrete set of input states, (iii) a corresponding set of measurements, and closing with the formula that reconstructs the scattering matrix from all these elements.

As shown in Fig. 1b, the setup consists of the scatterer to be analyzed—a point-like object, or any active or passive optical medium—, a photonic channel that couples the light in and out of the scatterer, a signal generator to prepare the input states, and a multi-port beam splitter that divides the output signal into N independent measurement ports.

Our protocol requires a specific set of input states to inject photons into the system. In particular, we assume coherent state wavepacket inputs $|\alpha_{\vec{k}}\rangle$, created on top of the vacuum [27] using a superposition of M generic bosonic modes $A_{k_j}^\dagger$ as

$$|\Psi_{\text{in}}\rangle = |\alpha_{\vec{k}}\rangle = e^{-\frac{1}{2}|\alpha|^2} \exp\left(\sum_{j=1}^M \alpha_{k_j} A_{k_j}^\dagger\right) |0\rangle, \quad (2)$$

where α_{k_j} are complex weights and $|\alpha|^2$ the mean photon number. In this work we consider wavepacket modes A_k^\dagger which are centered at momentum k , as well as plane waves, but the formalism admits other quantum numbers such as path or polarization [28]. In practice, these superposition coherent states can be prepared using a signal generator [cf. Fig. 1b], or alternatively with beam-splitters, as shown in Fig. 2 for a superposition of two components $A_{k_1}^\dagger$ and $A_{k_2}^\dagger$.

To perform the measurements, the output of the scatterer $|\Psi_{\text{out}}\rangle = U|\Psi_{\text{in}}\rangle$, is led through a balanced multi-port beam-splitter into N homodyne detection devices [see Fig. 1b]. At each output port ($r = 1 \dots N$), we filter outgoing photons with momentum p_r , and measure the quadratures X_{p_r} and P_{p_r} to reconstruct the Fock operators $B_{p_r} = X_{p_r} + iP_{p_r}$. The nature of the beam-splitter transformation is irrelevant: we just need that all detectors get a similar fraction of the scattered output, typically

$$B_{p_r} = N^{-1/2} A_{p_r} + (N-1 \text{ vacuum inputs}). \quad (3)$$

Combining the homodyne measurements we can therefore estimate any correlation function of the form

$$\langle B_{p_1} \dots B_{p_n} \rangle = N^{-n/2} \langle \alpha_{\vec{k}} | U^\dagger A_{p_1} \dots A_{p_n} U | \alpha_{\vec{k}} \rangle, \quad (4)$$

where the filtered momenta p_1, \dots, p_n will correspond to the outgoing indices in the scattering matrix that we wish to estimate (1). For N measurement ports, this will be limited to $n \leq N$.

Scattering matrix tomography protocol: After describing the input, scattering and measurement stages of our setup, we finally write down our reconstruction protocol:

Protocol 1 (General) *Let us assume a setup such as the one in Fig. 1b. In order to reconstruct the scattering matrix (1) with $n = 1 \dots N$ and $m = 1 \dots M$, we will prepare $2^M M$ input states $|\Psi_{\text{in}}(l, \vec{s})\rangle$, labeled by $l = 1 \dots 2M$,*

and $\vec{s} = (s_1, \dots, s_M)$. The different input states are defined as in Eq. (2) by separate choices of phases

$$\alpha_{k_j}^{l, \vec{s}} = s_j e^{i l \pi / M} |\alpha_{k_j}|, \quad \begin{cases} s_1 = 1 \\ s_{m \geq 2} = \pm 1 \end{cases}, \quad (5)$$

for the different components $j = 1 \dots M$. Then, for each of the input states, measure the values of the $2N$ quadratures and gather enough statistics to reconstruct the correlations $F_n(l, \vec{s}) = \langle \Psi_{\text{in}}(l, \vec{s}) | U^\dagger B_{p_1} \dots B_{p_n} U | \Psi_{\text{in}}(l, \vec{s}) \rangle$, for $n = 1 \dots N$. From all these values, the scattering matrix elements read

$$S_{p_1 \dots p_n k_1 \dots k_m} = \frac{N^{n/2} e^{|\alpha|^2}}{2^M M} \sum_{l=1}^{2M} \sum_{\vec{s}} \frac{F_n(l, \vec{s})}{\prod_{j=1}^m \alpha_{k_j}^{l, \vec{s}}} + \varepsilon_m, \quad (6)$$

with a small error $\varepsilon_m = \mathcal{O}(|\alpha|^2)$, for attenuated coherent state inputs $|\alpha| \ll 1$.

The derivation of this protocol, as well as all other demonstrations, are collected in the supplementary material (SM) [29]. It is important to remark that once we fix the number of measurement channels, N , and input modes, M , we can *simultaneously* reconstruct *all* scattering matrices from sizes 1×1 up to $N \times M$, using the *same* set of experiments.

Elastic scatterers: The reconstruction protocol is much simpler when the system conserves the total number of photons in scattering. This happens for scatterers with a single ground state, and Jaynes-Cummings type interactions with $U(1)$ symmetry (no cyclic transitions). In this case the scattering matrix (1) is zero whenever $n \neq m$, and quadrature measurements with different global input phases are equivalent. We can reduce the total number of measurement setups to 2^{M-1} and produce stricter bounds on the error:

Protocol 2 (Elastic scatterers) *When it is a priori known that the scatterer conserves the number of photons, follow the steps in Protocol 1, but reduce the choice of input states to $|\Psi_{\text{in}}(\vec{s})\rangle$, where $\vec{s} = (s_1, \dots, s_M)$ and*

$$\alpha_{k_j}^{\vec{s}} = s_j |\alpha_{k_j}|, \quad \begin{cases} s_1 = 1 \\ s_{j \geq 2} = \pm 1 \end{cases}, \quad (7)$$

$$F_n(\vec{s}) = \langle \Psi_{\text{in}}(\vec{s}) | U^\dagger B_{p_1} \dots B_{p_n} U | \Psi_{\text{in}}(\vec{s}) \rangle,$$

$$S_{p_1 \dots p_n k_1 \dots k_m} = \frac{N^{m/2} e^{|\alpha|^2}}{2^{M-1}} \sum_{\vec{s}} \frac{F_m(\vec{s})}{\prod_{j=1}^m \alpha_{k_j}^{\vec{s}}} + \varepsilon_m,$$

with the error bounded by $|\varepsilon_m| \leq \mathcal{O}(e^{|\alpha|^2} - 1)$.

Examples: Experiments with superconducting or optical qubits at low power are well described by a RWA Hamiltonian [11], and we can apply Protocol 2. For a single photon we require only one input with arbitrary, but small, complex amplitude α_{k_1} , and the measurement of one quadrature B_{p_1} , obtaining

$$S_{p_1 k_1} = \langle 0 | A_{p_1} U A_{k_1}^\dagger | 0 \rangle = e^{|\alpha|^2} \frac{\langle B_{p_1} \rangle}{\alpha_{k_1}} + \varepsilon_1. \quad (8)$$

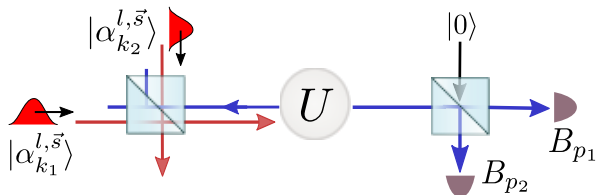


FIG. 2. Experimental setup for measuring $S_{p_1 k_1}$, $S_{p_1 p_2 k_1}$, $S_{p_1 k_1 k_2}$, and $S_{p_1 p_2 k_1 k_2}$, which requires two beam splitters, two coherent state wave-packet inputs with controlled phases, and two homodyne detection devices. At each input port of the left beam-splitter we prepare independent coherent state wavepackets, $|\alpha_{k_j}^{l,s}\rangle = \exp(-|\alpha_{k_j}|^2/2)\exp(\alpha_{k_j}^{l,s} A_{k_j}^\dagger)|0\rangle$, producing the desired superposition (2) towards the scatterer.

This formula includes the limit of state-of-the-art experiments [1, 2, 4], where the transmission and reflection coefficients, $S_{+k,+k}$ and $S_{-k,+k}$, are recovered from the ratio between the input amplitude α_k of a monochromatic coherent beam, and the scattered amplitude $\langle B_{\pm k} \rangle$.

The reconstruction of the two-photon scattering matrix demands at least two measurement ports, B_{p_1} and B_{p_2} , and a set of two input modes, $A_{k_1}^\dagger$ and $A_{k_2}^\dagger$. As shown in Fig. 2, an experiment could combine two independent pulses $A_{k_1}^\dagger$ and $A_{k_2}^\dagger$ through a beam splitter, and then direct the scattering output to two homodyne measurement devices for estimating the correlations $\langle B_{p_1} B_{p_2} \rangle$. For a RWA model, we reconstruct

$$S_{p_1 p_2 k_1 k_2} = e^{|\alpha|^2} \frac{[F_2(1,1) - F_2(1,-1)]}{|\alpha_{k_1}| |\alpha_{k_2}|} + \varepsilon_2, \quad (9)$$

using only two different input phases. If we cannot ensure $U(1)$ symmetry because of inelastic channels [21], ultrastrong coupling [18], external driving on the scatterer [30], etc., we will need a total of 8 input states with varying global phase $e^{i\ell\pi/2}$, and the general reconstruction formula (6). However, the same measurements will generate all the information to reconstruct the matrices $S_{p_1 k_1}$, $S_{p_1 k_1 k_2}$, $S_{p_1 p_2 k_1}$, and $S_{p_1 p_2 k_1 k_2}$.

Arbitrary reconstruction error: There are three sources of error in our reconstruction protocol: (i) quantum fluctuations, (ii) detector noise, and (iii) the approximation error ε_m . The first source of error scales as $\mathcal{O}(\mathcal{N}^{-1/2})$ and can be decreased arbitrarily by increasing the number of repetitions of the experiment \mathcal{N} . By design, our protocol is intrinsically resilient to the second source of errors, because detector noise averages out when combining odd powers of quadratures from different detectors—a fact used with great success in superconducting circuits [24–26]. Finally, we can also reduce the approximation error $|\varepsilon_m| \sim |\alpha|^2 \ll 1$, working with different low-power coherent states. The idea is to combine Z different estimates of the scattering matrix, $E(|\alpha|) = S + \mathcal{O}(|\alpha|^2)$, reconstructed for different average intensities $|\alpha|$, to create an estimate with a lower order

truncation error $\mathcal{O}(|\alpha|^{2Z})$. The simplest instance of this idea requires one extra estimate $E(2|\alpha|)$ as,

$$S = \frac{4}{3}E(|\alpha|) - \frac{1}{3}E(2|\alpha|) + \mathcal{O}(|\alpha|^4), \quad (10)$$

and higher order formulas can be derived iteratively [29].

The need of wavepackets: We will now argue that in the previous reconstruction it is essential to use finite length wavepackets as input states,

$$A_k^\dagger = \int dk' \psi_k(k') a_{k'}^\dagger, \quad (11)$$

built from normalized superpositions of plane waves a_k^\dagger , with $[a_k, a_{k'}^\dagger] = \delta(k - k')$ and $\int |\psi_k(k')|^2 dk' = 1$.

The use of pulsed light contrasts with existing theory, which computes the scattering matrix elements for well defined momentum modes [11, 12, 17], as in

$$\bar{S}_{p_1 \dots p_n k_1 \dots k_m} = \langle 0 | a_{p_1} \dots a_{p_n} U a_{k_1}^\dagger \dots a_{k_m}^\dagger | 0 \rangle. \quad (12)$$

The reasons for studying \bar{S} are (i) the possibility of analytical calculations and that (ii) it reveals the underlying nonlinearity of the scatterer. Take for instance the two-photon scattering matrix for a two-level system, which can be decomposed as [11, 31]

$$\bar{S}_{p_1 p_2 k_1 k_2} = \bar{S}_{p_1 k_1} \bar{S}_{p_2 k_2} + \bar{S}_{p_1 k_2} \bar{S}_{p_2 k_1} + i c \bar{\mathcal{T}}_{p_1 p_2 k_1 k_2} \delta(\omega_{p_1} + \omega_{p_2} - \omega_{k_1} - \omega_{k_2}), \quad (13)$$

with ω_k the photon dispersion relation and c the velocity of light. The first two terms in Eq. (13) connect independent single-photon events \bar{S}_{pk} , while the last one is a truly nonlinear contribution $\bar{\mathcal{T}}_{p_1 p_2 k_1 k_2}$ that describes photon-photon interaction mediated by simultaneous interaction with the scatterer, such as the two-photon Kerr effect [3].

Interestingly, S and \bar{S} are related by the integral equation,

$$S_{p_1 \dots p_n, k_1 \dots k_m} = \int \dots \int d^m k' d^n p' \bar{S}_{p'_1 \dots p'_n, k'_1 \dots k'_m} \times \prod_{j=1}^m \psi_{k_j}(k'_j) \prod_{r=1}^n \psi_{p_r}^*(p'_r), \quad (14)$$

which we will now evaluate for the two-photon scattering matrix in a tomography experiment using Gaussian pulses

$$\psi_k(k') = G_\sigma(k' - k)^{1/2}, \quad \text{with} \quad (15)$$

$$G_\sigma(k') = (\pi\sigma^2)^{-1/2} e^{-(k'/\sigma)^2}.$$

We are specially interested in analyzing how a nonlinearity such as $\bar{\mathcal{T}}$ in Eq. (13) manifests itself in the monochromatic limit of negligible bandwidth $\sigma \rightarrow 0$. To do so, we focus on forward scattering ($k_j, p_r > 0$) in

a waveguide with linear dispersion relation $\omega_k = c|k|$, but this can be easily extended [29]. The main result is that the *measured* two-photon scattering matrix $S_{p_1 p_2, k_1 k_2} = S_{p_1 k_1} S_{p_2 k_2} + S_{p_1 k_2} S_{p_2 k_1} + iT_{p_1 p_2, k_1 k_2}$ also splits into single- and two-photon contributions, which are given by the convolutions,

$$S_{p_1 k_1} = e^{-\frac{(p_1 - k_1)^2}{4\sigma^2}} \int dk'_1 G_\sigma(k'_1 - \frac{[k_1 + p_1]}{2}) t_{k'_1}, \quad (16)$$

$$T_{p_1 p_2, k_1 k_2} = 2\sigma\sqrt{\pi} e^{-(p_1 + p_2 - k_1 - k_2)^2 / (8\sigma^2)} \times \iint dp'_1 dk'_1 dk'_2 \mathcal{W}(p'_1, k'_1, k'_2) \bar{\mathcal{T}}_{p'_1 p'_2, k'_1 k'_2}. \quad (17)$$

The transmission coefficient $t_{k'_1}$ appears in Eq. (16) as a result of energy conservation, $\bar{S}_{pk} = t_p \delta(p - k)$, as well as the relation $p'_2 = k'_1 + k'_2 - p'_1$ for the integration momenta in Eq. (17). Because the kernel \mathcal{W} in Eq. (17) is a product of three Gaussians [29] and $\bar{\mathcal{T}}$ is typically a smooth and bounded function, any nonlinear contribution to the scattering experiment vanishes as we make the wavepacket width σ tend to zero,

$$S_{p_1 k_1} = \mathcal{O}(1), \quad T_{p_1 p_2, k_1 k_2} = \mathcal{O}(\sigma^1). \quad (18)$$

This argument can be extended to higher order processes, $T_{p_1 \dots p_n, k_1 \dots k_m} \sim \sigma^{(m+n-2)/2}$ [32], illustrating the fact that nonlinear terms can only be activated when photons coexist in the scatterer, and the probability of this overlap tends to zero as the wavepacket length $1/\sigma$ tends to infinity. We therefore conclude that an *efficient reconstruction of the full scattering matrix for two or more photons requires working with finite duration wavepackets*.

Deconvolution formulas: Even if we need wavepackets to get an experimentally measurable signal, we can still reconstruct the monochromatic properties from such experiments. We illustrate this by deriving the single- and two-photon forward scattering coefficients t_{k_1} and $\bar{\mathcal{T}}_{p_1 p_2, k_1 k_2}$ from the measured $S_{k_1 k_1}$ and $T_{p_1 p_2, k_1 k_2}$, using Gaussian wavepackets (15). This requires inverting Eqs. (16)-(17), which can be done analytically due to the Gaussian kernels [33–35]. For the single-photon transmission we obtain,

$$t_{k_1} = \int dk'_1 \mathcal{K}_\sigma(k'_1 - k_1) S_{k'_1 k'_1}, \quad \text{where} \\ \mathcal{K}_\sigma(k) = G_\sigma(k) \sum_{q=0}^{\infty} \frac{(-1)^q}{2^q q!} H_{2q} \left(\frac{k}{\sigma} \right). \quad (19)$$

The inverse kernel $\mathcal{K}_\sigma(k)$ contains Hermite polynomials $H_q(x) = (-1)^q e^{x^2} \partial_x^q (e^{-x^2})$ and produces a series that is convergent because $S_{k_1 k_1}$ decays exponentially fast. As discussed above, the single-photon reconstruction still works with monochromatic beams, recovering the state-of-the-art experimental formula $t_{k_1} = \lim_{\sigma \rightarrow 0} S_{k_1 k_1}$.

The reconstruction of the two-photon scattering strength $\bar{\mathcal{T}}$ from the measured values of T involves a

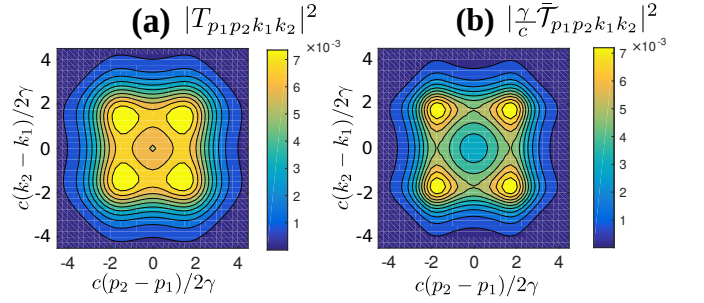


FIG. 3. Nonlinear part of the two-photon scattering matrix for a two-level system weakly coupled to a 1D photonic channel. (a) Predicted measurement of $|T_{p_1 p_2, k_1 k_2}|^2$ for incoming gaussian wavepackets centered at momenta $k_1, k_2 > 0$, and outgoing ones at momenta $p_1, p_2 > 0$. We vary the differences $k_2 - k_1$, $p_2 - p_1$, and keep the average $\bar{k} = (k_1 + k_2)/2 = (p_1 + p_2)/2$ fixed to $\bar{k} = (\omega_0 + 2\gamma)/c$, with ω_0 the transition frequency and γ the decay rate of the qubit. The width of the wavepackets is set to $\sigma = 0.5(\gamma/c)$. (b) Deconvolution of the measurements according to Eq. (20), to recover the two-photon interaction strength $\bar{\mathcal{T}}_{p_1 p_2, k_1 k_2}$ of the two-level scatterer derived in Refs. [10, 11].

three-dimensional deconvolution using a product of the same inverse kernels \mathcal{K}_σ [35]. Energy conservation imposes that the only nonzero elements of $\bar{\mathcal{T}}_{p_1 p_2, k_1 k_2}$ have to be functions of the average momentum $\bar{k} = (k_1 + k_2)/2 = (p_1 + p_2)/2$, and their relative differences, $\Delta_p = (p_2 - p_1)/2$ and $\Delta_k = (k_2 - k_1)/2$. For these elements we get,

$$\bar{\mathcal{T}}_{p_1 p_2, k_1 k_2} = \frac{1}{\sqrt{\pi}\sigma} \iiint d\bar{k}' d\Delta'_p d\Delta'_k T_{\bar{k}' - \Delta'_p, \bar{k}' + \Delta'_p, \bar{k}' - \Delta'_k, \bar{k}' + \Delta'_k} \\ \times \mathcal{K}_\sigma(\sqrt{2}[\bar{k}' - \bar{k}]) \mathcal{K}_\sigma(\Delta'_p - \Delta_p) \mathcal{K}_\sigma(\Delta'_k - \Delta_k). \quad (20)$$

As an illustration, we evaluate the measured scattering matrix T and the reconstructed monochromatic version $\bar{\mathcal{T}}$, for a gedanken experiment with Gaussian pulses and a two-level scatterer. This problem admits an analytical solution [10, 11] with which we can test the reconstruction formulas. As shown in Figs. 3a-b, the measured matrix T is broader than the monochromatic $\bar{\mathcal{T}}$, due to the convolution with the Gaussians. A good reconstruction demands an optimal wavepacket width σ : it cannot be too small, because T vanishes, and it cannot be too large, because the outgoing wavepackets will exceed the bandwidth of the homodyne device. We numerically find that the optimum lays around the linewidth of the two-level system itself, $\sigma \sim \gamma/c$, where γ is the spontaneous emission rate. This is the regime in which the nonlinear effects and the coexistence of photons in the qubit are both simultaneously maximized.

Summary and outlook: This Letter introduced a tomography protocol for reconstructing the scattering matrix of a photonic field interacting with a quantum scatterer, using coherent states and correlated homodyne measurements. We have demonstrated that pulsed spec-

troscopy is needed to gather information about the non-linear processes in scattering. This could remind the reader of two-dimensional pulsed spectroscopy methods in the optical and NMR realms [36, 37], but those constitute a time-resolved interrogation of the scatterer, whereas our protocol studies the asymptotic transformation (1) imparted by an optical medium in a propagating field.

While our protocol is inspired by recent progress in the fields of waveguide QED and nanophotonics, the idea, setup, and formulas can be used to probe any system which is in contact with a linear bosonic field. This includes not only superconducting qubits in strong-coupling [1, 3] or ultrastrong-coupling 1D setups [4], but also studying single molecule emitters in 3D [8], or other extended optical media. The reconstruction protocol is so general that it does not require any a-priori knowledge of the quantum emitter, and can be applied in the presence of decoherence and dissipation. We believe that under such circumstances our protocol is optimal, but particular symmetries or a better understanding of the models can lead to substantial simplifications [cf. Protocol 2] to be considered in future work.

The authors acknowledge support from MINECO/FEDER Project FIS2015-70856-P and CAM PRICYT Research Network QUITEMAD+ S2013/ICE-2801.

-
- [1] O. Astafiev, A. M. Zagoskin, A. A. Abdumalikov, Y. A. Pashkin, T. Yamamoto, K. Inomata, Y. Nakamura, and J. S. Tsai, *Science* **327**, 840 (2010).
- [2] I.-C. Hoi, C. M. Wilson, G. Johansson, T. Palomaki, B. Peropadre, and P. Delsing, *Phys. Rev. Lett.* **107**, 073601 (2011).
- [3] I.-C. Hoi, A. F. Kockum, T. Palomaki, T. M. Stace, B. Fan, L. Tornberg, S. R. Sathyamoorthy, G. Johansson, P. Delsing, and C. M. Wilson, *Phys. Rev. Lett.* **111**, 053601 (2013).
- [4] P. Forn-Díaz, J. J. García-Ripoll, B. Peropadre, J.-L. Orgiazzi, M. A. Yurtalan, R. Belyansky, C. M. Wilson, and A. Lupascu, *Nature Phys.* **13**, 39 (2017).
- [5] T. G. Tiecke, J. D. Thompson, N. P. de Leon, L. R. Liu, V. Vuletić, and M. D. Lukin, *Nature* **508**, 241 (2014).
- [6] A. Goban, C.-L. Hung, J. D. Hood, S.-P. Yu, J. A. Muniz, O. Painter, and H. J. Kimble, *Phys. Rev. Lett.* **115**, 063601 (2015).
- [7] M. Arcari, I. Söllner, A. Javadi, S. Lindskov Hansen, S. Mahmoodian, J. Liu, H. Thyrrestrup, E. H. Lee, J. D. Song, S. Stobbe, and P. Lodahl, *Phys. Rev. Lett.* **113**, 093603 (2014).
- [8] J. Hwang, M. Pototschnig, R. Lettow, G. Zumofen, A. Renn, S. Götzinger, and V. Sandoghdar, *Nature* **460**, 76 (2009).
- [9] J. T. Shen and S. Fan, *Opt. Lett.* **30**, 2001 (2005).
- [10] J.-T. Shen and S. Fan, *Phys. Rev. A* **76**, 062709 (2007).
- [11] S. Fan, S. E. Kocabaş, and J.-T. Shen, *Phys. Rev. A* **82**, 063821 (2010).
- [12] T. Caneva, M. T. Manzoni, T. Shi, J. S. Douglas, J. I. Cirac, and D. E. Chang, *New J. Phys.* **17**, 113001 (2015).
- [13] M. Pletyukhov and V. Gritsev, *New J. Phys.* **14**, 095028 (2012).
- [14] M. Laakso and M. Pletyukhov, *Phys. Rev. Lett.* **113**, 183601 (2014).
- [15] D. L. Hurst and P. Kok, *arXiv:1705.07016* (2017).
- [16] T. Shi and C. P. Sun, *Phys. Rev. B* **79**, 205111 (2009).
- [17] T. Shi, D. E. Chang, and J. I. Cirac, *Phys. Rev. A* **92**, 053834 (2015).
- [18] T. Shi, Y. Chang, and J. J. García-Ripoll, *arXiv:1701.04709* (2017).
- [19] M. Pechal, J.-C. Besse, M. Mondal, M. Oppliger, S. Gasparinetti, and A. Wallraff, *Phys. Rev. Applied* **6**, 024009 (2016).
- [20] B. Peropadre, D. Zueco, D. Porras, and J. J. García-Ripoll, *Phys. Rev. Lett.* **111**, 243602 (2013).
- [21] M. Goldstein, M. H. Devoret, M. Houzet, and L. I. Glazman, *Phys. Rev. Lett.* **110**, 017002 (2013).
- [22] A. Kurcz, A. Bermudez, and J. J. García-Ripoll, *Phys. Rev. Lett.* **112**, 180405 (2014).
- [23] A. V. Gorshkov, J. Otterbach, E. Demler, M. Fleischhauer, and M. D. Lukin, *Phys. Rev. Lett.* **105**, 060502 (2010).
- [24] E. P. Menzel, F. Deppe, M. Mariani, M. A. Araque Caballero, A. Baust, T. Niemczyk, E. Hoffmann, A. Marx, E. Solano, and R. Gross, *Phys. Rev. Lett.* **105**, 100401 (2010).
- [25] R. D. Candia, E. P. Menzel, L. Zhong, F. Deppe, A. Marx, R. Gross, and E. Solano, *New J. Phys.* **16**, 015001 (2014).
- [26] M. P. da Silva, D. Bozyigit, A. Wallraff, and A. Blais, *Phys. Rev. A* **82**, 043804 (2010).
- [27] Throughout this work we assume that the scatterer has a unique initial and final states, which are implicit in the definition of $|0\rangle$, but this restriction can be easily lifted.
- [28] In any of these cases, the normalization of the coherent state (2) implies that the mean photon number is given by $|\alpha|^2 = \sum_{j,j'=1}^M \alpha_{k_j}^* \alpha_{k_{j'}} f_{jj'}$, where the commutators $[A_{k_j}, A_{k_{j'}}^\dagger] = f_{jj'} \mathbb{I}$ are not orthonormal for wavepackets.
- [29] For more details, see the supplementary material for “Multi-photon scattering tomography with coherent states”.
- [30] L. S. Bishop, J. M. Chow, J. Koch, A. A. Houck, M. H. Devoret, E. Thuneberg, S. M. Girvin, and R. J. Schoelkopf, *Nature Phys.* **5**, 105 (2009).
- [31] S. Xu, E. Rephaeli, and S. Fan, *Phys. Rev. Lett.* **111**, 223602 (2013).
- [32] This derives from Eq. (14) by a purely dimensional analysis, assuming $\psi_k(k') = \tilde{\psi}_k(k'/\sigma)/\sigma^{1/2}$, and a monochromatic nonlinear contribution $\tilde{S} \sim \bar{T} \delta(\sum_r \omega_{p_r} - \sum_j \omega_{k_j})$ that satisfies energy conservation as in Eq. (13).
- [33] T.-M. Fang, S.-S. Shei, R. J. Nagem, and G. v. H. Sandri, *Il Nuovo Cimento B* **109**, 83 (1994).
- [34] W. Ulmer and W. Kaissl, *Physics in Medicine and Biology* **48**, 707 (2003).
- [35] W. Ulmer, *Inverse Problems* **26**, 085002 (2010).
- [36] D. Keusters, H.-S. Tan, and Warren, *The Journal of Physical Chemistry A* **103**, 10369 (1999).
- [37] M. Cho, *Chemical Reviews* **108**, 1331 (2008).

Supplemental Material for: Multi-photon scattering tomography with coherent states

Tomás Ramos and Juan José García-Ripoll

Instituto de Física Fundamental IFF-CSIC, Calle Serrano 113b, Madrid 28006, Spain

I. SCATTERING TOMOGRAPHY RELATIONS

In this section, we derive the central relations underlying our multi-photon scattering tomography protocol. We relate the components of an unknown unitary matrix U with the measurement of certain photonic quadrature correlations at the output, when probing the system with coherent state inputs (see Fig. 4). The associated error is shown to be negligible in the limit that the coherent state probes are highly attenuated, and we even find a strict upper bound for it in the case the scattering conserves the photon number.

We split the derivation in two parts. First, in Sec. I.A, we show how to reconstruct the scattering matrix elements in the total photon number basis, namely

$$S_{nm} = \langle 0|A^n U(A^\dagger)^m|0\rangle. \quad (21)$$

These matrix elements describe m incoming to n outgoing photons, without resolving internal properties of the photons such as momentum, frequency, polarization, etc. Then, in Sec. I.B, we extend the protocol to resolve a photonic degree of freedom k , and show how to reconstruct the general scattering matrix elements,

$$S_{p_1 \dots p_n k_1 \dots k_m} = \langle 0|A_{p_1} \dots A_{p_n} U A_{k_1}^\dagger \dots A_{k_m}^\dagger |0\rangle. \quad (22)$$

This applies to m incoming photons with quantum numbers k_1, \dots, k_m to n outgoing with p_1, \dots, p_n , and requires the preparation of more complicated coherent state inputs with a signal generator (see Fig. 4b). To filter the different quantum numbers p_1, \dots, p_n at the output, we make use of a multi-port beam-splitter which decomposes the signal into independent channels (see Fig. 4b). Interestingly, this scheme allows us to measure the output correlations in a way that is insensitive to detector noise, as explained in the main text.

A. Tomography of a scattering matrix in the photon number basis

We start by considering the situation sketched in Fig. 4a, where photons propagate along a one-dimensional (1D) channel and interact with an unknown quantum medium according to a scattering matrix U . As a result, any photonic input state $|\Psi_{\text{in}}\rangle$ is transformed into the output $|\Psi_{\text{out}}\rangle = U|\Psi_{\text{in}}\rangle$, with the only restriction that the vacuum state $|0\rangle$ remains invariant, i. e. $U|0\rangle = |0\rangle$. Besides this last condition, the unitary U

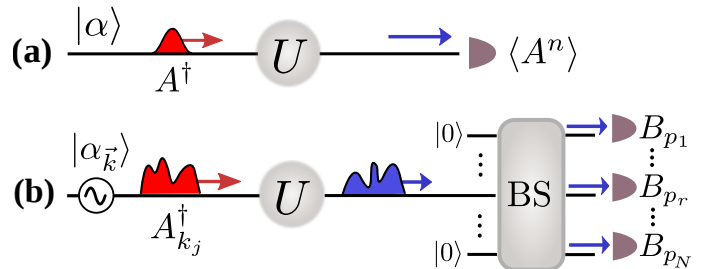


FIG. 4. Multi-photon scattering tomography protocol. (a) We input an attenuated coherent state $|\alpha\rangle$ and measure quadrature moments $\langle A^n \rangle$ at the output, to determine the scattering matrix elements in the total number basis (21). (b) To have additional resolution on a photon quantum number k (22), we need to input a coherent state superposition $|\alpha_{\vec{k}}\rangle$ with different values of this quantity $\vec{k} = (k_1, \dots, k_M)$, and measure the quadrature correlations $\langle B_{p_1} \dots B_{p_n} \rangle$ at the $n = 1, \dots, N$ independent outputs of a beam-splitter.

is completely arbitrary, and we show in the following how to reconstruct its elements using homodyne detection.

First, our scattering tomography protocol requires the preparation of coherent state input,

$$|\Psi_{\text{in}}\rangle = |\alpha\rangle = e^{-\frac{1}{2}|\alpha|^2} e^{\alpha A^\dagger} |0\rangle, \quad (23)$$

where A^\dagger is a bosonic creation operator of a photon in the channel, satisfying $[A, A^\dagger] = \mathbb{I}$, and $\alpha = |\alpha|e^{i\phi}$ is the complex vacuum displacement with module $|\alpha|$ and phase ϕ .

Secondly, we require the measurement of photon output correlations of the form

$$\langle A^n \rangle = \langle \Psi_{\text{out}}|A^n|\Psi_{\text{out}}\rangle = \langle \alpha|U^\dagger A^n U|\alpha\rangle, \quad (24)$$

which can be determined to any order n by measuring the output quadratures X and P via homodyne detection, with $A = X + iP$.

To derive the relation between the scattering matrix elements (21) and the correlations (24), let us first consider the measurement of a general operator Q at the output, namely $\langle Q \rangle = \langle \alpha|U^\dagger Q U|\alpha\rangle$. If we replace here the definition of the coherent state (23) and decompose α in terms of its module and phase, we obtain

$$\langle Q \rangle = e^{-|\alpha|^2} \sum_{t=0}^{\infty} \sum_{r=\lambda}^{\infty} |\alpha|^{r+t} e^{i\phi(r-t)} C_{tr}. \quad (25)$$

where the coefficients C_{tr} read,

$$C_{tr} = \frac{\langle 0|A^t U^\dagger Q U (A^\dagger)^r |0\rangle}{t!r!}. \quad (26)$$

In addition, λ can only take two values: $\lambda = 1$ in the special case $Q|0\rangle = 0$ (since then $C_{t_0} = 0$), and $\lambda = 0$ in any other case. In particular, for the choice $Q = A^n$ we can take $\lambda = 1$, but we keep the derivation general.

Our aim now is to solve for the coefficients of the form $C_{0m} = \langle 0|U^\dagger Q U (A^\dagger)^m |0\rangle/m!$ from Eq. (25), since they correspond to the scattering matrix elements (21) when $Q = A^n$. As we show in the following, we can isolate the coefficients C_{0m} , for $m = \lambda, \dots, M$, by preparing $R = 2(M+1-\lambda)$ different coherent input states $|\alpha(l)\rangle$ of the form (23), and measuring $\langle Q\rangle(l) = \langle \alpha(l)|U^\dagger Q U |\alpha(l)\rangle$ for each of them ($l = 1, \dots, R$). Importantly, we choose the different coherent state inputs $|\alpha(l)\rangle$ to have the same module $|\alpha|$, but different global phase ϕ_l as $\alpha(l) = |\alpha|e^{i\phi_l}$. As a result, we can replace $\langle Q\rangle \rightarrow \langle Q\rangle(l)$ and $\phi \rightarrow \phi_l$ in Eq. (25), obtaining a set of $l = 1, \dots, R$ independent equations for the unknowns C_{tr} , which read

$$\langle Q\rangle(l) = e^{-|\alpha|^2} \sum_{t=0}^{\infty} \sum_{r=\lambda}^{\infty} |\alpha|^{r+t} e^{i\phi_l(r-t)} C_{tr}. \quad (27)$$

To see how to choose the phases ϕ_l in order to solve for the coefficients C_{0m} in Eq. (27), let us multiply Eq. (27) by $e^{|\alpha|^2} e^{-im\phi_l}/R$ and sum over all values $l = 1, \dots, R$, obtaining the equation,

$$\frac{e^{|\alpha|^2}}{R} \sum_{l=1}^R \frac{\langle Q\rangle(l)}{e^{im\phi_l}} = \sum_{u=\lambda}^{\infty} \sum_{d=-u+2\lambda}^u |\alpha|^u T_{ud} \sum_{l=1}^R \frac{e^{i\phi_l(d-m)}}{R}, \quad (28)$$

after the convenient change of variables, $u = r + t$ and $d = r - t$. We have defined the new coefficients,

$$T_{ud} = C_{(u-d)/2, (u+d)/2}, \quad (29)$$

and the sum over d , denoted with a bold sum symbol $\sum_{y=a}^b$, corresponds to a sum where y goes from a to b in steps of 2. Choosing the phases as

$$\phi_l = (2\pi l)/R, \quad (30)$$

we see that the last factor on the right hand side of Eq. (28) becomes the discrete Fourier transform of a periodic Kronecker delta,

$$\frac{1}{R} \sum_{l=1}^R e^{(2i\pi l/R)(d-m)} = \delta_{d, m+qR}, \quad (31)$$

with q taking any integer value due to the function periodicity of size R . When replacing (31) into Eq. (28), we see that all non-vanishing terms must satisfy $d = m+qR$, with $q \in \mathbb{Z}$ and d of the same parity as u . This allows us to select specific terms in the sum. In particular, if we set

$$R = 2(M+1-\lambda), \quad (32)$$

then all non-zero terms with $u \leq M+1$ in Eq. (28) can only take $d = m$ or equivalently $q = 0$, as they all lie

within the first period of the delta function. In addition, since d is bounded by $-u + 2\lambda \leq d \leq u$, then all terms with $u < m \leq M$ vanish, and our target coefficients C_{0m} appear to lowest non-zero order $\sim |\alpha|^m$, for $m = \lambda, \dots, M$, namely

$$\frac{e^{|\alpha|^2}}{R} \sum_{l=1}^R \frac{\langle Q\rangle(l)}{e^{im\phi_l}} = |\alpha|^m C_{0m} + \sum_{u=m+2}^{\infty} |\alpha|^u \sum_{q=q_{\min}}^{q_{\max}} T_{u, m+qR}. \quad (33)$$

Here, the bounds of q are given by $q_{\min} = -I[(u+m-2\lambda)/R]$ and $q_{\max} = I[(u-m)/R]$ where the function $I[x]$ rounds the number x to its nearest smaller integer. From Eq. (33) it is clear that in the case of highly attenuated coherent state inputs,

$$|\alpha| \ll 1, \quad (34)$$

all terms on order $\sim |\alpha|^{m+2}$ or higher can be neglected and we can solve for C_{0m} with a small relative error. By formally solving for the coefficient C_{0m} in Eq. (33), we obtain the main result of this subsection,

$$C_{0m} = \frac{\langle 0|Q U (A^\dagger)^m |0\rangle}{m!} = \frac{e^{|\alpha|^2}}{R} \sum_{l=1}^R \frac{\langle Q\rangle(l)}{[\alpha(l)]^m} + \epsilon_m, \quad (35)$$

which relates the desired matrix elements $\langle 0|Q U (A^\dagger)^m |0\rangle$, for powers $m = \lambda, \dots, M$, with the measurements $\langle Q\rangle(l) = \langle \alpha(l)|U^\dagger Q U |\alpha(l)\rangle$ at the output. In particular, when replacing $Q = A^n$ in Eq. (35), we access all the scattering matrix elements $S_{nm} = \langle 0|A^n U (A^\dagger)^m |0\rangle$ in Eq. (21), describing $m = \lambda, \dots, M$ incident photons to any number n of outgoing photons in the channel A . As $Q|0\rangle = A^n|0\rangle = 0$, we can take $\lambda = 1$ and the number of measurements needed is $R = 2M$.

Regarding the relative error ϵ_m , we find a precise expression for it in terms of a series with even powers of the coherent state amplitude $|\alpha|$ as,

$$\epsilon_m = \sum_{v=1}^{\infty} |\alpha|^{2v} h_{vm}. \quad (36)$$

From here it is clear that ϵ_m scales as $|\epsilon_m| \sim |\alpha|^2 \ll 1$ for highly attenuated coherent states. The coefficients h_{vm} are independent of the coherent input power, and are given in general by,

$$h_{vm} = - \sum_{q=q_{\min}}^{q_{\max}} T_{2v+m, m+qR}. \quad (37)$$

In addition, using Eqs. (26), (29), (36) and (37), as well as the triangular inequality, we can show that the relative error (36) is strictly bounded by $|\epsilon_m| \leq \sum_{v=1}^{\infty} |\alpha|^{2v} |h_{vm}|$, where the bound for the coefficients reads

$$|h_{vm}| \leq \sum_{q=q_{\min}}^{q_{\max}} \frac{|\langle v - qR/2 | U^\dagger Q U | v + m + qR/2 \rangle|}{\sqrt{(v+m+qR/2)!(v-qR/2)!}}, \quad (38)$$

with $|v\rangle = (A^\dagger)^v/\sqrt{v!}$ the photon number states.

It is worth highlighting the special case where we *a priori* know that the number of photons is conserved during the scattering, i. e. $[U, A^\dagger A] = 0$, since then the tomography protocol is strongly simplified. In particular, only the diagonal components S_{mm} are nonzero and a single measurement, $R = 1$, is enough to determine them. To see this, notice that the conservation of photon number and $Q = A^m$ implies that T_{ud} is only nonzero for $d = m$. Therefore, replacing $T_{ud} = C_{(u-m)/2, (u+m)/2} \delta_{dm}$ in Eq. (28), allows us to derive the same Eqs. (33) and (35), but now valid for $R = 1$ and all $m = 1, \dots, \infty$, as all coefficients appearing at lower order than $\sim |\alpha|^m$ are zero in this case, regardless the value of R . Another peculiarity of this elastic scattering case is that the bound for the relative error in Eq. (38) takes a very simple closed form. Again, using $Q = A^m$ and the conservation of photon number, we can set $U|v\rangle = e^{i\varphi v}|v\rangle$ and $q = 0$ in Eq. (38), and additionally using $A^m|v\rangle = \sqrt{v!/(v-m)!}|v-m\rangle$, we find a simple bound for the coefficients in this elastic case,

$$|h_{vm}| \leq 1/v!. \quad (39)$$

As a result, the error ϵ_m in Eq. (36) is strictly bounded by a displaced exponential for all m , namely

$$|\epsilon_m| \leq \sum_{v=1}^{\infty} \frac{|\alpha|^{2v}}{v!} = e^{|\alpha|^2} - 1. \quad (40)$$

B. Tomography of a scattering matrix with resolution on a photon degree of freedom

In this subsection, we extend the protocol to measure scattering matrix elements with resolution on a photon quantum number k as in Eq. (22). First, in Sec. I.B.1. , we generalize Eq. (35) to determine matrix elements of the form $\langle 0|QUA_{k_1}^\dagger \dots A_{k_m}^\dagger|0\rangle$, which describe input states of m photons with different quantum numbers k_1, \dots, k_m . Then, in Sec. I.B.2. , we give details on a beam-splitter setup to measure the output quadrature correlations $\langle B_{p_1} \dots B_{p_n} \rangle$ (see Fig. 4b), and we show how to reconstruct the general scattering matrix elements (22) from these correlations.

1. Superposition coherent state input

First, we need a mechanism to inject photons, with various values of a quantum number k , at the input of the scatterer (see Fig. 4b). To this end we prepare a coherent state input $|\alpha_{\vec{k}}\rangle$ as in Eq. (23), but now for a superposition mode $A_{\vec{k}}^\dagger$, defined for M different compo-

nents $\vec{k} = (k_1, \dots, k_M)$ as

$$A_{\vec{k}}^\dagger = \sum_{j=1}^M \xi_j A_{k_j}^\dagger. \quad (41)$$

Here, $A_{k_j}^\dagger$ for $j = 1, \dots, M$, are the creation operators of a photon with degree of freedom k_j , and ξ_j is a projection vector normalized as $\sum_{j,v=1}^M \xi_j^* \xi_v [A_{k_j}, A_{k_v}^\dagger] = \mathbb{I}$, such that $[A_{\vec{k}}, A_{\vec{k}}^\dagger] = \mathbb{I}$. Notice that the modes A_{k_j} do not satisfy standard commutation relations in general, allowing us to describe single photon wavepackets as inputs. For instance, for gaussian wavepacket modes as defined in Eqs. (11) and (15) of the main text, we obtain $[A_{k_j}, A_{k_v}^\dagger] = e^{-(k_j - k_v)^2 / (2\sigma)^2} \mathbb{I}$.

The coherent state input corresponding to the superposition mode (41) can be expressed more explicitly as

$$|\Psi_{\text{in}}\rangle = |\alpha_{\vec{k}}\rangle = e^{-\frac{1}{2}|\alpha|^2} e^{\alpha A_{\vec{k}}^\dagger} |0\rangle \quad (42)$$

$$= e^{-\frac{1}{2}|\alpha|^2} \exp\left(\sum_{j=1}^M \alpha_{k_j} A_{k_j}^\dagger\right) |0\rangle, \quad (43)$$

where the weights on each component are given by $\alpha_{k_j} = \alpha \xi_j$, with $\alpha = |\alpha|e^{i\phi}$, and the mean photon number reads $|\alpha|^2 = \sum_{j,v=1}^M \alpha_{k_j}^* \alpha_{k_v} [A_{k_j}, A_{k_v}^\dagger]$. This superposition coherent state can be prepared using a signal generator (see Fig. 4b), which is readily implemented in microwave and optical photonic setups.

When we vary the global phase of the displacement weights as $\alpha_{k_j}(l) = |\alpha|e^{i\phi_l} \xi_j$, with $l = 1, \dots, R$ and ϕ_l defined in the previous subsection, we can apply the result (35) to the superposition operator in Eq. (41), and thereby determine the matrix elements $\langle 0|QU(A_{\vec{k}}^\dagger)^m|0\rangle$, with the associated error $\epsilon_m \sim |\alpha|^2$, for $|\alpha| \ll 1$. However, this is not enough to determine matrix elements of the form $\langle 0|QUA_{k_1}^\dagger \dots A_{k_m}^\dagger|0\rangle$, since when expanding the multinomial in $\langle 0|QU(A_{\vec{k}}^\dagger)^m|0\rangle$, we see that it contains many unwanted terms, namely

$$\begin{aligned} \langle 0|QU(A_{\vec{k}}^\dagger)^m|0\rangle &= \sum_{\substack{n_1, \dots, n_M=1 \\ \sum n_j = m}}^M \frac{m!(\xi_1)^{n_1} \dots (\xi_M)^{n_M}}{n_1! \dots n_M!} \quad (44) \\ &\quad \times \langle 0|QU(A_{k_1}^\dagger)^{n_1} \dots (A_{k_M}^\dagger)^{n_M}|0\rangle. \end{aligned}$$

Notice that the sums over n_1, \dots, n_M are constrained to values that satisfy $\sum_{j=1}^M n_j = m$, as demanded by the multinomial theorem.

Our aim in this subsection is therefore to extract from the above relation the term $\langle 0|QUA_{k_1}^\dagger \dots A_{k_m}^\dagger|0\rangle$ and relate it to $\langle 0|QU(A_{\vec{k}}^\dagger)^m|0\rangle$ by canceling all unwanted terms. We achieve this by performing additional measurements as in the previous subsection, but now we vary the relative phases in the superposition mode

$A_k^\dagger(\vec{s}) = \sum_{j=1}^M \xi_j^{(s_j)} A_{k_j}^\dagger$ as $\xi_j^{(s_j)} = e^{i\Theta_j^{(s_j)}} |\xi_j|$. Here, $\Theta_j^{(s_j)}$ for $s_j = 1, \dots, R_j$ denote the R_j different values that the phase of each component $j = 1, \dots, M$ can take, and we keep all the moduli $|\xi_j|$ fixed. We also use the shorthand notation, $\vec{s} = (s_1, \dots, s_M)$, to arrange the values of the M different indices. To see how to choose the phases

$\Theta_j^{(s_j)}$ in order to cancel the unwanted terms in Eq. (44), we divide it by $m! \xi_1^{(s_1)} \dots \xi_m^{(s_m)}$ and sum over all independent values of \vec{s} , for $s_j = 1, \dots, R_j$, and $j = 1, \dots, M$, obtaining

$$\sum_{s_1=1}^{R_1} \dots \sum_{s_M=1}^{R_M} \frac{\langle 0|QU[A_k^\dagger(\vec{s})]^m|0\rangle}{m! \xi_1^{(s_1)} \dots \xi_m^{(s_m)}} = \sum_{\substack{n_1, \dots, n_M=1 \\ \sum_j n_j=m}}^M \frac{\langle 0|QU(A_{k_1}^\dagger)^{n_1} \dots (A_{k_M}^\dagger)^{n_M}|0\rangle}{n_1! \dots n_M!} \prod_{j=1}^m |\xi_j|^{n_j-1} \sum_{s_j=1}^{R_j} e^{i\Theta_j^{(s_j)}(n_j-1)} \prod_{v=m+1}^M |\xi_v|^{n_v} \sum_{s_v=1}^{R_v} e^{i\Theta_v^{(s_v)} n_v}. \quad (45)$$

Choosing $\Theta_j^{(s_j)} = 2\pi(s_j - 1)/R_j$, for all $j = 1, \dots, M$, we can use the same property (31) as in the previous subsection and form periodic Kronecker deltas in Eq. (45),

$$\sum_{s_j=1}^{R_j} e^{i\Theta_j^{(s_j)}(n_j-t_j)} = R_j \delta_{n_j, t_j + q_j R_j}, \quad (46)$$

with q_j and t_j arbitrary integers. Importantly, due to the constrains $n_j \geq 0$ and $\sum_j n_j = m$, when choosing R_j as

$$R_{j \geq 2} = 2, \quad \text{and} \quad R_1 = 1, \quad (47)$$

then the deltas in Eq. (45) manage to cancel all terms, except for the one with $n_1 = \dots = n_m = 1$ and $n_{m+1} = \dots = n_R = 0$, obtaining the desired relation,

$$\langle 0|QUA_{k_1}^\dagger \dots A_{k_m}^\dagger|0\rangle = \sum_{s_2, \dots, s_M=1}^2 \frac{\langle 0|QU[A_k^\dagger(\vec{s})]^m|0\rangle}{\xi_1^{(1)} \xi_2^{(s_2)} \dots \xi_m^{(s_m)} m! 2^{M-1}}. \quad (48)$$

With the choice (47), we see that the relative phases take the simple values $\Theta_{j \geq 2}^{(1,2)} = (0, \pi)$ and $\Theta_1^{(1)} = 0$, resulting only in sign changes of the vector components as, $\xi_{j \geq 2}^{(1,2)} = \pm |\xi_j|$ and $\xi_1^{(1)} = |\xi_1|$. Therefore, from now on and also in the main text, we conveniently redefine the indices $\vec{s} = (s_1, \dots, s_M)$ as

$$s_{j \geq 2} = \pm 1, \quad \text{and} \quad s_1 = 1, \quad (49)$$

such that the different values of vector components are simply given by

$$\xi_j^{(s_j)} = s_j |\xi_j|. \quad (50)$$

Finally, replacing the result (35) into Eq. (48), we obtain a closed relation for the matrix elements $\langle 0|QUA_{k_1}^\dagger \dots A_{k_m}^\dagger|0\rangle$, with $m = \lambda, \dots, M$, and the various measurements $\langle Q \rangle(l, \vec{s}) = \langle \alpha_{\vec{k}}(l, \vec{s}) | U^\dagger QU | \alpha_{\vec{k}}(l, \vec{s}) \rangle$,

given by

$$\langle 0|QUA_{k_1}^\dagger \dots A_{k_m}^\dagger|0\rangle = \frac{e^{|\alpha|^2}}{2^{M-1} R} \sum_{l=1}^R \sum_{\vec{s}} \frac{\langle Q \rangle(l, \vec{s})}{\prod_{j=1}^m \alpha_{k_j}^{l, \vec{s}}} + \varepsilon_m. \quad (51)$$

Here, we have used the new notation (49) for \vec{s} , and defined the weights $\alpha_{k_j}^{l, \vec{s}}$ of the coherent states $|\alpha_{\vec{k}}(l, \vec{s})\rangle$ in Eq. (43) as

$$\alpha_{k_j}^{l, \vec{s}} = \alpha(l) \xi_j^{(s_j)} = s_j e^{i\phi_l} |\xi_j| |\alpha| = s_j e^{i\phi_l} |\alpha_{k_j}|, \quad (52)$$

with $l = 1, \dots, R$, and ϕ_l as previously defined in Eqs. (30) and (32).

The relative error in Eq. (51) is also of the form,

$$\varepsilon_m = \sum_{v=1}^{\infty} |\alpha|^{2v} f_{vm}, \quad (53)$$

with the modified error coefficients f_{vm} given by

$$f_{vm} = \frac{1}{2^{M-1}} \sum_{\vec{s}} \frac{h_{vm}(\vec{s})}{\prod_{j=1}^m \xi_j^{(s_j)}}, \quad (54)$$

where $h_{vm}(\vec{s})$, defined in Eq. (37), now depend on \vec{s} via $A_{\vec{k}}^\dagger(\vec{s})$ in the coefficients $T_{ud}(\vec{s})$. The modified error ε_m is bounded by

$$|\varepsilon_m| \leq \frac{1}{\prod_{j=1}^m |\xi_j|} \sum_{v=1}^{\infty} |\alpha|^{2v} \sum_{\vec{s}} \frac{|h_{vm}(\vec{s})|}{2^{M-1}}, \quad (55)$$

with $|h_{vm}(\vec{s})|$ bounded by Eq. (38) that now depends on \vec{s} in general.

2. Homodyne detection at beam-splitter outputs

Notice that Eq. (51) directly gives the desired scattering matrix elements,

$$S_{p_1 \dots p_n k_1 \dots k_m} = \langle 0|A_{p_1} \dots A_{p_n} U A_{k_1}^\dagger \dots A_{k_m}^\dagger|0\rangle, \quad (56)$$

in the case we replace $Q = A_{p_1} \dots A_{p_n}$. Using the resulting relation, however, demands the measurement of specific correlation functions at the scatterer's output on channel A , namely

$$\langle A_{p_1} \dots A_{p_n} \rangle = \langle \alpha_{\vec{k}} | U^\dagger A_{p_1} \dots A_{p_n} U | \alpha_{\vec{k}} \rangle. \quad (57)$$

To distinguish the contribution of photons with different quantum numbers p_1, \dots, p_n in the above correlations (57), a filtering mechanism at the scatterer's output is needed. Therefore, we connect the output of the scatterer to a multi-port beam-splitter, which divides the scattered signal into N independent channels (see Fig. 4b). At each independent output port of the beam-splitter, labeled by $r = 1, \dots, N$, we measure the quadratures X_{p_r} and P_{p_r} , and reconstruct the field operator $B_{p_r} = X_{p_r} + iP_{p_r}$ for outgoing photons with quantum number p_r . When gathering enough statistics via homodyne detection, we can determine the correlations,

$$\langle B_{p_1} \dots B_{p_n} \rangle = \langle \alpha_{\vec{k}} | U^\dagger B_{p_1} \dots B_{p_n} U | \alpha_{\vec{k}} \rangle, \quad (58)$$

which can be related to the correlations in Eq. (57) via the beam-splitter transformation U_{BS} .

Notice that the specific form of the beam-splitter transformation U_{BS} is irrelevant, as long as each output port r gets a similar fraction of the scattered signal $B_{p_r} \sim A_{p_r}$ and that all other $N - 1$ input ports are in vacuum (see Fig. 4). As a practical example, let us consider the transformation for a balanced multi-port beam-splitter, for which the photonic amplitude operators at each independent output, $r = 1, \dots, N$, read

$$B_{p_r} = \frac{1}{\sqrt{N}} A_{p_r} + \frac{1}{\sqrt{N}} \sum_{r'=1}^{N-1} e^{(2i\pi/N)rr'} \Upsilon_{p_r}^{r'}. \quad (59)$$

Here, $\Upsilon_p^{r'}$ with $r' = 1, \dots, N - 1$ denote the annihilation operators on the $N - 1$ vacuum input ports different than channel A . As these extra channels are independent between each other and with channel A , they satisfy the commutation relations, $[\Upsilon_k^{r'}, \Upsilon_p^{r'}] = \delta_{rr'} \delta_{pk}$, and $[A_k, \Upsilon_p^{r'}] = [U, \Upsilon_p^{r'}] = 0$, implying $[B_{p_r}, B_{p_r'}^\dagger] = \delta_{rr'}$.

Using expression (59) in Eq. (58), we see that the required correlations (57) can be accessed by measuring at the outputs of the beam-splitter. In fact, both correlations are just proportional to each other:

$$\langle A_{p_1} \dots A_{p_n} \rangle = N^{n/2} \langle B_{p_1} \dots B_{p_n} \rangle. \quad (60)$$

Finally, we just replace $Q = A_{p_1} \dots A_{p_n}$ into Eq. (51) and use the relation (60) to obtain the general scattering matrix elements $S_{p_1 \dots p_n k_1 \dots k_m}$ in terms of the measurable correlations $F_n(l, \vec{s}) = \langle \alpha_{\vec{k}}(l, \vec{s}) | U^\dagger B_{p_1} \dots B_{p_n} U | \alpha_{\vec{k}}(l, \vec{s}) \rangle$, as

$$S_{p_1 \dots p_n k_1 \dots k_m} = \frac{\sqrt{N^n} e^{|\alpha|^2}}{2^{M-1} R} \sum_{l=1}^R \sum_{\vec{s}} \frac{F_n(l, \vec{s})}{\prod_{j=1}^m \alpha_{k_j}^{l, \vec{s}}} + \varepsilon_m. \quad (61)$$

This is the main result of the paper and is shown in Eqs. (6) and (7) of the main text, for the general ($R = 2M$) and elastic ($R = 1$) cases, respectively.

The truncation error ε_m appearing in the final result (61) has a closed analytical upper bound in the case that the scattering matrix U conserves the number of photons (Protocol 2 of the main text). From Eq. (55) we see that this problem is equivalent to find a closed bound for the coefficients $|h_{vm}(\vec{s})|$. Therefore, we replace $Q = A_{p_1} \dots A_{p_m}$ in Eq. (38) and use Eq. (59), to re-express the bound in terms of the B_{p_r} operators as

$$|h_{vm}(\vec{s})| \leq \sum_{q=q_{\min}}^{q_{\max}} \frac{|\langle v - q \frac{R}{2} | U^\dagger B_{p_1} \dots B_{p_m} U | v + m + q \frac{R}{2} \rangle|}{N^{-m/2} \sqrt{(v + m + q \frac{R}{2})! (v - q \frac{R}{2})!}}. \quad (62)$$

Since U conserves the total number of photons, we can set $q = 0$ and $U|v\rangle = e^{i\varphi_v}|v\rangle$ in Eq. (62), and additionally using the Cauchy-Schwarz inequality, we obtain

$$|h_{vm}(\vec{s})| \leq \frac{|\langle v + m | (B_{p_1}^\dagger B_{p_1}) \dots (B_{p_m}^\dagger B_{p_m}) | v + m \rangle|^{1/2}}{N^{-m/2} \sqrt{(v + m)! v!}}. \quad (63)$$

The next step is to decompose the total number state $|v + m\rangle$ into components along all N channels of the interferometer, and using the fact the the sum of photons in all channels is fixed, $N = \sum_{r=1}^N B_{p_r}^\dagger B_{p_r}$, we can bound the numerator in Eq. (63) by $\sqrt{(v + m)! v!}$. Using this result in Eq. (63) we obtain a simple bound for the coefficients similar to Eq. (39),

$$|h_{vm}(\vec{s})| \leq \frac{N^{m/2}}{v!}, \quad (64)$$

and replacing this in Eq. (53), we finally find the strict bound for the error,

$$|\varepsilon_m| \leq \frac{N^{m/2} (e^{|\alpha|^2} - 1)}{\prod_{j=1}^m |\xi_j|}. \quad (65)$$

Notice that since the first term on the right hand side of Eq. (61) also scales as $N^{m/2} / (\prod_{j=1}^m |\xi_j|)$, the relative error is actually bounded by $\mathcal{O}(e^{|\alpha|^2} - 1)$ as stated in the Protocol 2 of the main text.

II. REDUCTION OF TRUNCATION ERROR BY MULTIPLE ESTIMATES OF THE SCATTERING MATRIX

An intrinsic error that limits the precision of our tomography protocol is the *truncation error* $\varepsilon_m = \sum_{v=1}^{\infty} |\alpha|^{2v} f_{vm}$, which scales as $|\varepsilon_m| \sim \mathcal{O}(|\alpha|^2)$ for attenuated coherent state inputs, $|\alpha| \ll 1$.

In this section, we show how to reduce the scaling of this error to arbitrary order $\sim \mathcal{O}(|\alpha|^{2Z})$, by performing

the scattering tomography protocol in Eq. (61) at Z different laser input powers $|\alpha|$, and combining the resulting estimates in a clever way.

A first order estimate $E(|\alpha|)$ of the scattering matrix S is given by the outcome of our protocol in Eq. (61) as,

$$E(|\alpha|) = \frac{\sqrt{N^n} e^{|\alpha|^2}}{2^{M-1} R} \sum_{l=1}^R \sum_{\vec{s}} \frac{F_n(l, \vec{s})}{\prod_{j=1}^m \alpha_{k_j}^{l, \vec{s}}} \quad (66)$$

$$= S - \sum_{v=1}^{\infty} |\alpha|^{2v} f_{vm}, \quad (67)$$

which has a precision $E(|\alpha|) = S + \mathcal{O}(|\alpha|^2)$, for $|\alpha| \ll 1$. Interestingly, if we consider another first order estimate measured at twice the power $E(2|\alpha|)$, we can combine it with Eq. (67) and cancel the error term of leading order $\sim |\alpha|^2$. As a result, we obtain a second order estimate with higher precision, $E^{(2)}(|\alpha|) = S + \mathcal{O}(|\alpha|^4)$, given by

$$E^{(2)}(|\alpha|) = \frac{4E(|\alpha|) - E(2|\alpha|)}{3}, \quad (68)$$

$$= S - \sum_{v=2}^{\infty} |\alpha|^{2v} f_{vm}^{(2)}, \quad (69)$$

where the modified error coefficients read $f_{vm}^{(2)} = f_{vm}(4 - 4^v)/3$. In general, this process can be iterated up to arbitrary order using the recursion relation,

$$E^{(\mu)} = \frac{4^{\mu-1} E^{(\mu-1)}(|\alpha|) - E^{(\mu-1)}(2|\alpha|)}{4^{\mu-1} - 1}, \quad (70)$$

which gives the estimate of order μ from two estimates of a lower order: $E^{\mu-1}(|\alpha|)$ and $E^{\mu-1}(2|\alpha|)$. The μ -order estimate has a precision $E^{(\mu)}(|\alpha|) = S + \mathcal{O}(|\alpha|^{2\mu})$, and its associated error is explicitly given by

$$E^{(\mu)}(|\alpha|) = S - \sum_{v=\mu}^{\infty} |\alpha|^{2v} f_{vm}^{(\mu)}, \quad (71)$$

where the μ -order coefficients $f_{vm}^{(\mu)}$ are obtained recursively by

$$f_{vm}^{(\mu)} = \frac{(4^{\mu-1} - 4^v)}{(4^{\mu-1} - 1)} f_{vm}^{(\mu-1)}. \quad (72)$$

The final step is to express an estimate of arbitrary order $E^{(Z)}(|\alpha|)$ in terms of first order estimates only, as these are the ones that we measure in practice via (66). Using $Z - 1$ times the recursion relation (70), it is straightforward to check that a Z -order estimate $E^{(Z)}(|\alpha|)$ requires Z different first order estimates $E(x_q)$, measured at laser powers $x_q = 2^{q-1}|\alpha|$, with $q = 1, \dots, Z$. Then, combining these Z first order estimates, we obtain

$$E^{(Z)}(|\alpha|) = \sum_{q=1}^Z w_q^{(Z)} E(x_q), \quad (73)$$

where the coefficients $w_q^{(Z)}$ are determined from the iterations with Eqs. (68) and (71). As an example, for $Z = 1, \dots, 4$, the coefficients are explicitly given by

$$w_q^1 = 1, \quad (74)$$

$$w_q^2 = \frac{1}{3}(4, -1), \quad (75)$$

$$w_q^3 = \frac{1}{45}(64, -20, 1), \quad (76)$$

$$w_q^4 = \frac{1}{2835}(4096, -1344, 84, -1). \quad (77)$$

In summary, the scattering matrix elements of S can be measured with a precision $\sim |\alpha|^{2Z} \ll 1$ by combining Z first order estimates (66), obtained at different laser powers as

$$S_{p_1 \dots p_n k_1 \dots k_m} = \sum_{q=1}^Z w_q^{(Z)} E(x_q) + \mathcal{O}(|\alpha|^{2Z}), \quad \text{with} \quad (78)$$

$$E(x_q) = 2^{q-1} |\alpha|, \quad |\alpha| \ll 1, \quad q = 1, \dots, Z.$$

III. DECONVOLUTION WITH GAUSSIAN WAVEPACKETS IN DISPERSIVE CHANNELS

As explained in the main text, our scattering protocol requires wavepacket input modes,

$$A_k^\dagger = \int dk' \psi_k(k') a_{k'}^\dagger, \quad (79)$$

to be sensitive to nonlinear multi-photon scattering events. As a result, we have direct experimental access to the ‘wavepacket’ scattering matrix elements only, $S_{p_1 \dots p_n k_1 \dots k_m} = \langle 0 | A_{p_1} \dots A_{p_n} U A_{k_1}^\dagger \dots A_{k_m}^\dagger | 0 \rangle$, but the monochromatic counterparts, $\bar{S}_{p_1 \dots p_n k_1 \dots k_m} = \langle 0 | a_{p_1} \dots a_{p_n} U a_{k_1}^\dagger \dots a_{k_m}^\dagger | 0 \rangle$, can still be accessed by inverting the integral relation shown in Eq. (14) of the main text.

In this section, we show how to analytically solve the deconvolution integral for the monochromatic single- and two-photon scattering matrices in Eq. (13) of the main text. To do so, we assume wave-packets with gaussian shape and a possibly dispersive photonic channel, as shown below.

A. Gaussian deconvolution in a dispersive channel

As we want to discuss photons in a dispersive channel, the deconvolution integrals turn out to be simpler when working with frequency modes instead of momentum. Therefore, in this subsection we derive all deconvolution formulas in terms of frequency-direction modes, and in the next subsection we map the results to momentum, connecting to the specific formulas shown in the main text.

In the special case that the dispersion relation is symmetric, $\omega_k = \omega_{-k}$, and the group velocity is antisymmetric, $v_k = -v_{-k}$, the propagating momentum modes a_k can be unambiguously related to frequency-direction modes a_ω^ρ , as

$$a_\omega^\rho = \frac{a_{\rho|k|}}{\sqrt{|v_k|}}. \quad (80)$$

Here, the mapping assumes that photons with $k > 0$ propagate to the right ($v_k > 0$), while photons with $k < 0$ propagate to the left ($v_k < 0$), and we identify these directions with the quantum number $\rho = \text{sign}(k) = \pm$. In addition, the frequency ω of the photons has a one-to-one correspondence with the wavenumber $|k|$ via the invertible function $\omega = \omega_{|k|}$. Note that this relation (80) is not valid for $k = 0$, since the group velocity necessarily vanishes $v_0 = 0$. Nevertheless, we will always consider propagating wavepackets (79) with negligible components on this $k = 0$ mode.

The wavepacket operators in Eq. (79) can be expressed in terms of frequency-direction modes as

$$A_k^\dagger = A_{\rho|k|}^\dagger = A_\omega^{\rho\dagger} = \sum_{\rho'} \int d\omega' \tilde{\psi}_\omega^{\rho\rho'}(\omega') a_{\omega'}^{\rho'\dagger}, \quad (81)$$

where the corresponding wavepacket profile is related to its momentum counterpart by

$$\tilde{\psi}_\omega^{\rho\rho'}(\omega') = \frac{\psi_k(k')}{\sqrt{|v_{k'}|}}. \quad (82)$$

In particular, we choose wavepackets with a gaussian profile defined as

$$\psi_\omega^{\rho\rho'}(\omega') = \sqrt{G_{\tilde{\sigma}}(\omega - \omega')} \delta_{\rho\rho'}, \quad \text{with} \quad (83)$$

$$G_{\tilde{\sigma}}(\omega') = (\pi\tilde{\sigma}^2)^{-1/2} e^{-(\omega'/\tilde{\sigma})^2}, \quad (84)$$

such that the wavepacket mode $A_\omega^{\rho\dagger} = \int d\omega' G_{\tilde{\sigma}}(\omega' - \omega)^{1/2} a_{\omega'}^{\rho\dagger}$ is built exclusively from monochromatic frequency modes $a_{\omega'}^\rho$ propagating in the same direction ρ . We also assume that the central frequency of the wavepacket ω is much larger than its width, $\tilde{\sigma} \ll \omega$, to ensure a vanishing component on the non-propagating mode $\omega = 0$.

Using all these considerations, we can re-express the general integral equation (14) of the main text, in terms of frequency-direction modes, as

$$\begin{aligned} S_{\omega_1 \dots \omega_n \nu_1 \dots \nu_m}^{\rho_1 \dots \rho_n \eta_1 \dots \eta_m} &= \int \dots \int d^m \nu' d^n \omega' \bar{S}_{\omega'_1 \dots \omega'_n \nu'_1 \dots \nu'_m}^{\rho_1 \dots \rho_n \eta_1 \dots \eta_m} \times \\ &\times \prod_{j=1}^m G_{\tilde{\sigma}}(\nu'_j - \nu_j)^{1/2} \prod_{r=1}^n G_{\tilde{\sigma}}(\omega'_r - \omega_r)^{1/2}, \end{aligned} \quad (85)$$

where $\bar{S}_{\omega'_1 \dots \omega'_n \nu'_1 \dots \nu'_m}^{\rho_1 \dots \rho_n \eta_1 \dots \eta_m} = \langle 0 | a_{\omega'_1}^{\rho_1} \dots a_{\omega'_n}^{\rho_n} U a_{\nu'_1}^{\eta_1 \dagger} \dots a_{\nu'_m}^{\eta_m \dagger} | 0 \rangle$ denote the monochromatic scattering elements from m incoming photons with frequencies ν_1, \dots, ν_m , and directions η_1, \dots, η_m , to n outgoing ones with frequencies $\omega_1, \dots, \omega_n$, and directions ρ_1, \dots, ρ_n , respectively.

In the following, we specialize the discussion to the single- and two-photon matrix elements of a scatterer with a single ground state. In this case, the conservation of energy allows us to decompose the monochromatic scattering components as in Eq. (13) of the main text:

$$\bar{S}_{\omega_1 \nu_1}^{\rho_1 \eta_1} = \chi_{\omega_1}^{\rho_1 \eta_1} \delta(\omega_1 - \nu_1), \quad (86)$$

$$\begin{aligned} \bar{S}_{\omega_1 \omega_2 \nu_1 \nu_2}^{\rho_1 \rho_2 \eta_1 \eta_2} &= \bar{S}_{\omega_1 \nu_1}^{\rho_1 \eta_1} \bar{S}_{\omega_2 \nu_2}^{\rho_2 \eta_2} + \bar{S}_{\omega_1 \nu_2}^{\rho_1 \eta_2} \bar{S}_{\omega_2 \nu_1}^{\rho_2 \eta_1} \\ &+ i \bar{T}_{\omega_1 \omega_2 \nu_1 \nu_2}^{\rho_1 \rho_2 \eta_1 \eta_2} \delta(\omega_1 + \omega_2 - \nu_1 - \nu_2). \end{aligned} \quad (87)$$

Here, $\chi_\omega^{\rho\eta}$ contain the reflection $r_\omega = \chi_\omega^{-\rho, \rho}$ and transmission $t_\omega = \chi_\omega^{\rho, \rho}$ coefficients, and the nonlinear contribution $\bar{T}_{\omega_1 \omega_2 \nu_1 \nu_2}^{\rho_1 \rho_2 \eta_1 \eta_2}$ describes photon-photon interactions mediated by the scatterer.

Using Eqs. (86)-(87) in Eq. (85), simplifies the integral relations by reducing their dimensionality. In particular, the single-photon scattering matrix satisfies,

$$S_{\omega_1 \nu_1}^{\rho_1 \eta_1} = e^{-\frac{(\omega_1 - \nu_1)^2}{4\tilde{\sigma}^2}} \int d\omega'_1 \chi_{\omega'_1}^{\rho_1 \eta_1} G_{\tilde{\sigma}}(\omega'_1 - \frac{[\omega_1 + \nu_1]}{2}). \quad (88)$$

On the other hand, the two-photon ‘wavepacket’ scattering matrix can be also decomposed into linear and nonlinear contributions,

$$S_{\omega_1 \omega_2 \nu_1 \nu_2}^{\rho_1 \rho_2 \eta_1 \eta_2} = S_{\omega_1 \nu_1}^{\rho_1 \eta_1} S_{\omega_2 \nu_2}^{\rho_2 \eta_2} + S_{\omega_1 \nu_2}^{\rho_1 \eta_2} S_{\omega_2 \nu_1}^{\rho_2 \eta_1} + iT_{\omega_1 \omega_2 \nu_1 \nu_2}^{\rho_1 \rho_2 \eta_1 \eta_2}, \quad (89)$$

where the non-linear part reads,

$$\begin{aligned} T_{\omega_1 \omega_2 \nu_1 \nu_2}^{\rho_1 \rho_2 \eta_1 \eta_2} &= 2\tilde{\sigma} \sqrt{\pi} e^{-\frac{(\bar{\omega} - \bar{\nu})^2}{2\tilde{\sigma}^2}} \int d\bar{\omega}' d\Delta'_\omega d\Delta'_\nu \mathcal{W}(\bar{\omega}', \Delta'_\omega, \Delta'_\nu) \\ &\times \bar{T}_{\bar{\omega}' - \Delta'_\omega, \omega' + \Delta'_\omega, \omega' - \Delta'_\nu, \omega' + \Delta'_\nu}^{\rho_1 \rho_2 \eta_1 \eta_2}. \end{aligned} \quad (90)$$

Here, the kernel \mathcal{W} is the product of three Gaussians,

$$\mathcal{W} = G_{\tilde{\sigma}}(\sqrt{2}[\bar{\omega}' - \frac{(\bar{\omega} + \bar{\nu})}{2}]) G_{\tilde{\sigma}}(\Delta'_\omega - \Delta_\omega) G_{\tilde{\sigma}}(\Delta'_\nu - \Delta_\nu), \quad (91)$$

and we conveniently defined the new variables $\bar{\omega} = (\omega_1 + \omega_2)/2$, and $\bar{\nu} = (\nu_1 + \nu_2)/2$, $\Delta_\nu = (\nu_2 - \nu_1)/2$, and $\Delta_\omega = (\omega_2 - \omega_1)/2$.

Interestingly, both Eqs. (88) and (90) can be analytically inverted as they involve a product of Gaussian kernels for independent integration variables. Therefore, following Refs. [33–35] of the main text, we obtain

$$\chi_{\omega'_1}^{\rho_1 \eta_1} = \int d\omega_1 \mathcal{K}_{\tilde{\sigma}}(\omega_1 - \omega'_1) S_{\omega_1 \omega'_1}^{\rho_1 \eta_1}, \quad (92)$$

$$\begin{aligned} \bar{T}_{\omega_1 \omega_2 \nu_1 \nu_2}^{\rho_1 \rho_2 \eta_1 \eta_2} &= \frac{1}{\tilde{\sigma} \sqrt{\pi}} \int d\bar{\omega}' d\Delta'_\omega d\Delta'_\nu T_{\bar{\omega}' - \Delta'_\omega, \omega' + \Delta'_\omega, \omega' - \Delta'_\nu, \omega' + \Delta'_\nu}^{\rho_1 \rho_2 \eta_1 \eta_2} \\ &\times \mathcal{K}_{\tilde{\sigma}}(\sqrt{2}[\bar{\omega}' - \bar{\omega}]) \mathcal{K}_{\tilde{\sigma}}(\Delta'_\omega - \Delta_\omega) \mathcal{K}_{\tilde{\sigma}}(\Delta'_\nu - \Delta_\nu), \end{aligned} \quad (93)$$

where the inverse Gaussian kernel $\mathcal{K}_{\tilde{\sigma}}(\omega)$ is given by

$$K_{\tilde{\sigma}}(\omega) = G_{\tilde{\sigma}}(\omega) \sum_{q=0}^{\infty} \frac{(-1)^q}{2^q q!} H_{2q} \left(\frac{\omega}{\tilde{\sigma}} \right). \quad (94)$$

Here, $H_q(x) = (-1)^q e^{x^2} \partial_x^q (e^{-x^2})$ are Hermite polynomials and the series is convergent because $S_{\omega_1 \omega_1}^{\rho_1 \eta_1}$ and $T_{\omega_1 \omega_2 \nu_1 \nu_2}^{\rho_1 \rho_2 \eta_1 \eta_2}$ decay exponentially fast.

These last Eqs. (92)-(93) are direct analytical relations for the single- and two-photon scattering coefficients in terms of the ‘wavepacket’ counterparts, measurable with our tomography protocol. Moreover, they are valid for any dispersive photonic channel, satisfying $\omega_k = \omega_{-k}$ and $v_k = -v_{-k}$. In the next subsection, we connect to the expressions stated in the main text, by transforming to momentum variables, and specializing to a linear dispersion relation $\omega_k = c|k|$.

B. Gaussian deconvolution in momentum modes for a non-dispersive channel

The monochromatic scattering elements in momentum and frequency basis can be related using Eq. (80) as

$$\bar{S}_{p_1 k_1} = |v_{p_1} v_{k_1}|^{1/2} \bar{S}_{\omega_1 \nu_1}^{\rho_1 \eta_1}, \quad (95)$$

$$\bar{S}_{p_1 p_2 k_1 k_2} = |v_{p_1} v_{p_2} v_{k_1} v_{k_2}|^{1/2} \bar{S}_{\omega_1 \omega_2 \nu_1 \nu_2}^{\rho_1 \rho_2 \eta_1 \eta_2}, \quad (96)$$

where we used the identifications, $\omega_j = \omega_{p_j}$, $\nu_j = \omega_{k_j}$, $\rho_j = \text{sign}(p_j)$, and $\eta_j = \text{sign}(k_j)$. In addition, using the explicit formulas (86)-(87), we obtain the same formulas for the momentum monochromatic elements in the main

text,

$$\bar{S}_{p_1 k_1} = c \chi_{p_1 k_1} \delta(\omega_{p_1} - \omega_{k_1}), \quad (97)$$

$$\begin{aligned} \bar{S}_{p_1 p_2 k_1 k_2} &= \bar{S}_{p_1 k_1} \bar{S}_{p_2 k_2} + \bar{S}_{p_1 k_2} \bar{S}_{p_2 k_1} \\ &+ i c \bar{T}_{p_1 p_2 k_1 k_2} \delta(\omega_{p_1} + \omega_{p_2} - \omega_{k_1} - \omega_{k_2}), \end{aligned} \quad (98)$$

but now with the coefficients given for dispersive media as,

$$\chi_{p_1 k_1} = \frac{1}{c} |v_{p_1} v_{k_1}|^{1/2} \chi_{\omega_{p_1}}^{\rho_1 \eta_1}, \quad (99)$$

$$\bar{T}_{p_1 p_2 k_1 k_2} = \frac{1}{c} |v_{p_1} v_{p_2} v_{k_1} v_{k_2}|^{1/2} \bar{T}_{\omega_{p_1} \omega_{p_2} \omega_{k_1} \omega_{k_2}}^{\rho_1 \rho_2 \eta_1 \eta_2}. \quad (100)$$

The wavepacket profile used in Eq. (84) to perform the deconvolutions, can be recast in momentum as

$$\psi_k(k') = \left[\frac{|v_{k'}|}{c} G_\sigma \left(\frac{\omega_{k'} - \omega_k}{c} \right) \right]^{1/2} \delta_{\text{sign}(k), \text{sign}(k')}, \quad (101)$$

where the $\sigma = \tilde{\sigma}/c$ is the momentum width used in the main text.

Finally, when evaluating the above expressions for a linear dispersion relation $\omega_k = c|k|$ and forward scattering $k_j, p_j > 0$, as in the main text. In particular, the wavepacket profile reduces simply to $\psi_k(k') = G_\sigma(k' - k)^{1/2}$ and the scattering coefficients read,

$$t_{p_1} = \chi_{\omega_{p_1}}^{++} = \int dp'_1 \mathcal{K}_\sigma(p'_1 - p_1) S_{p'_1 p_1}, \quad (102)$$

$$\begin{aligned} \bar{T}_{p_1 p_2 k_1 k_2} &= \frac{1}{\sqrt{\pi} \sigma} \int d\bar{k}' d\Delta'_p d\Delta'_k T_{\bar{k}' - \Delta'_p, \bar{k}' + \Delta'_p, \bar{k}' - \Delta'_k, \bar{k}' + \Delta'_k} \\ &\times \mathcal{K}_\sigma(\sqrt{2}[\bar{k}' - \bar{k}]) \mathcal{K}_\sigma(\Delta'_p - \Delta_p) \mathcal{K}_\sigma(\Delta'_k - \Delta_k), \end{aligned} \quad (103)$$

where $\bar{k} = (k_1 + k_2)/2 = (p_1 + p_2)/2$, $\Delta_p = (p_2 - p_1)/2$ and $\Delta_k = (k_2 - k_1)/2$.